



Vibrational predissociation spectroscopy and theory of Ar-tagged, protonated Imidazole (Im) $\text{Im}_{1-3}\text{H}^+\cdot\text{Ar}$ clusters

Helen K. Gerardi^a, George H. Gardenier^a, Usha Viswanathan^b, Scott M. Auerbach^{b,*}, Mark A. Johnson^{a,*}

^a Department of Chemistry, Yale University, New Haven, CT 06520-8107, USA

^b Department of Chemistry, University of Massachusetts Amherst, Amherst, MA 01003, USA

ARTICLE INFO

Article history:

Received 7 June 2010

In final form 28 October 2010

Available online 31 October 2010

ABSTRACT

We report vibrational predissociation spectra and theoretical analysis of the Ar-tagged cluster ions of imidazole, $\text{Im}_{1-3}\text{H}^+\cdot\text{Ar}$. The frequencies of the external N–H stretches are observed to incrementally blue-shift toward that of neutral imidazole upon addition of the second and third Im molecules, consistent with the calculated behavior of the Im_3H^+ complex in which the excess charge is symmetrically shared by two internal N–H–N hydrogen bonds. A very strong, symmetrical doublet near 1000 cm^{-1} is observed for the Im_2H^+ complex and attributed to the parallel bridging proton displacement based on anharmonic frequency calculations.

© 2010 Published by Elsevier B.V.

1. Introduction

The transport of protons through molecular networks continues to receive considerable attention due to its importance in signal conduction [1,2] and fuel cell performance [3,4]. Although water often serves as the active medium, (e.g., in trans-membrane proton pumps and proton exchange membranes) [3–7], the high-temperature demand of fuel cell technology is driving the development of alternative, anhydrous platforms. Attractive candidates for this purpose are imidazole (Im) and its derivatives [8], where proton transfer occurs between the nitrogen atoms of two neighboring molecules via the making and breaking of covalent bonds. The key motifs in this scenario are the proton-bound dimers and trimers of Im, $\text{Im}_{2,3}\text{H}^+$, as these correspond to the elementary species at the heart of the proton-transport process. In fact, a 2009 theoretical analysis of proton transport in liquid Im by Voth and co-workers [9] used the calculated properties of $\text{Im}_{1-3}\text{H}^+$ clusters to parameterize the empirical valence bond model central to their approach. While there is a clear demand for experimental observables with which to calibrate such computational efforts, structural aspects of floppy ionic systems like Im_nH^+ have proven difficult to extract due to the diffuse bands obtained from measurements carried out directly in the condensed phase [10]. Recent advances [11] in gas-phase ion chemistry, however, have revealed sharp transitions for many such systems which can be compared directly with *ab initio* predictions of the spectra associated with various calculated minimum-energy structures.

* Corresponding authors. Fax: +1 413 545 4490 (S.M. Auerbach), +1 203 432 6144 (M.A. Johnson).

E-mail addresses: auerbach@chem.umass.edu (S.M. Auerbach), mark.johnson@yale.edu (M.A. Johnson).

In this Letter, we use Ar-cluster-based ion chemistry [12] to synthesize Ar-tagged Im_nH^+ ion clusters in the gas phase. We then characterize their structures by analyzing the vibrational band patterns, obtained using predissociation spectroscopy, in the context of predictions reported previously based on electronic structure calculations [13–16]. These theoretical results are supplemented where necessary by our own work to address the vibrational level structure expected for the potential energy surfaces in play.

The structure and microhydration behavior of imidazolium, ImH^+ , have been considered in detail previously by Dopfer and co-workers [14,17], with calculated equilibrium geometries of the Im^+ and ImH^+ cations reproduced in Figure 1. Note that ImH^+ adopts a C_{2v} configuration, providing two equivalent N–H binding sites for H-bond acceptors. In the microhydration study [14], these acidic protons were attached to two solvating water molecules to form the $\text{ImH}^+(\text{H}_2\text{O})_2$ cluster, where the excess charge is delocalized over the two N–H groups. Because Im has a much higher proton affinity than that of water, (943 and 691 kJ/mol, respectively) [18], the dihydrate is expected to conform to a solvated ImH^+ ‘core ion’.

The situation regarding the excess charge distribution becomes more interesting when instead of H_2O , Im molecules are bound to ImH^+ so that the excess proton is distributed among equivalent bases. A theoretical study by Tatara et al. [15] in 2003 addressed the structure and harmonic vibrational spectra of the proton-bound dimer, and concluded that the minimum energy arrangement (see Figure 2a) occurred with the excess proton closer to one Im molecule (i.e., in a double-minimum potential) and the Im rings oriented roughly orthogonal to one another. Yan et al. [16] then considered the effect of a third Im molecule, and recovered the chain structure displayed in Figure 2b, where again the two flanking Im molecules are rotated symmetrically almost

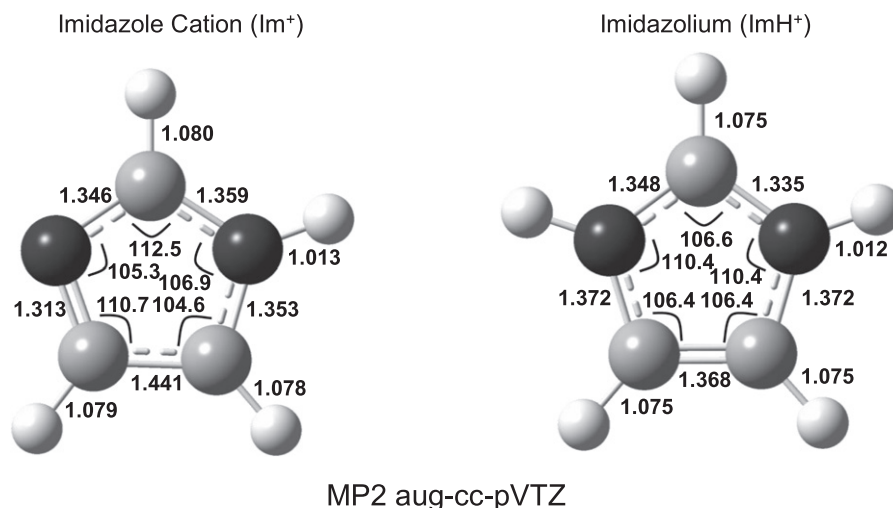


Figure 1. Calculated minimum-energy structures (MP2/aug-cc-pVTZ) of cationic imidazole (Im^+) and protonated imidazole, imidazolium (ImH^+). Hydrogen atoms are presented as white spheres, nitrogen atoms as black, and carbon atoms as gray.

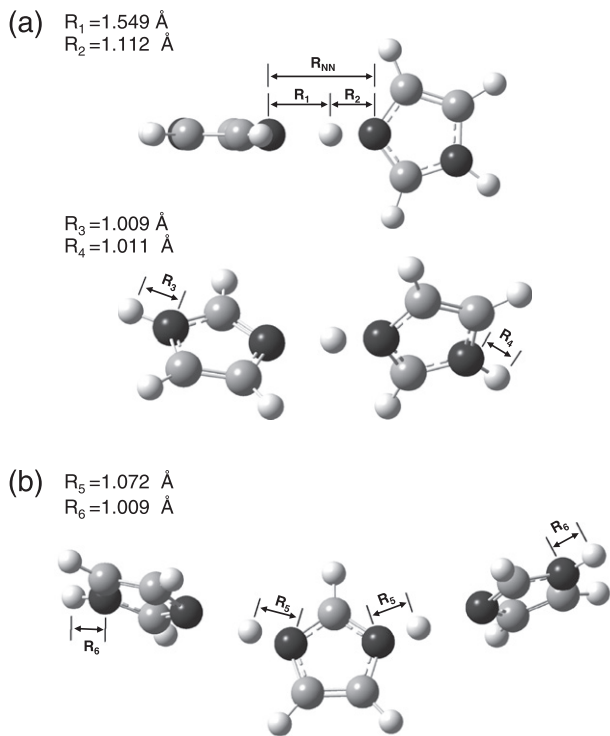


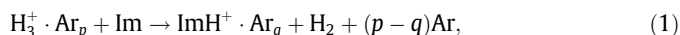
Figure 2. Calculated minimum-energy structures (B3LYP level, 6-311G(d,p) basis set) of (a) the protonated imidazole dimer (Im_2H^+), and (b) the protonated imidazole trimer (Im_3H^+). Two depictions of the protonated imidazole dimer are given in (a) to illustrate the roughly 90° angle between the planes of the two rings.

perpendicular to the plane defined by the central ImH^+ molecule. This structure can be viewed as an ‘imidazolium-like’ core, reminiscent of the microhydration behavior [14] reported earlier, but with substantially longer N–H bonds (by 0.04 Å) when the water molecules are replaced by Im.

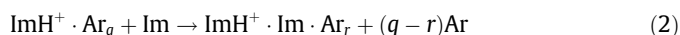
Key features of interest in homodromic H-bonded chains such as those predicted for Im_nH^+ clusters include the disposition of excess charge along the embedded N–H–N bonds and the concomitant distortion of each Im molecule according to its location along the chain. Here we investigate how these effects are encoded in the vibrational spectra of Im_nH^+ complexes.

2. Experimental and theoretical methods

The experimental spectra obtained in this study were recorded on the Yale tandem time-of-flight photofragmentation spectrometer described in detail previously [19]. Cationic argon clusters were generated by supersonically expanding roughly 40 psi of argon through the 0.5 mm-nozzle of a pulsed valve (Parker Hannifin). Imidazole clusters were formed in the source region by introducing trace vapor from a vessel of solid imidazole (melting point = 90°C) heated between 100 – 120°C , which was located close to the orifice of the free jet on the high-pressure side [12]. Synthesis of protonated, Ar-tagged imidazole clusters was accomplished by mixing $\sim 1\%$ H_2 with argon gas before expansion into the vacuum chamber, forming a distribution of H_3^+ molecular ions with large numbers of attached Ar atoms, $\text{H}_3^+ \cdot \text{Ar}_p$ ($p = 1$ – 20). These primary ions were then converted to protonated imidazole clusters through Ar-mediated proton transfer:

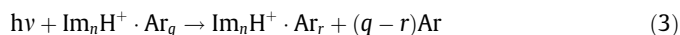


and condensation:



as indicated by the mass spectrum of the resulting cluster distribution shown in Figure 3. Production of the argon-tagged cationic imidazole, $\text{Im}^+ \cdot \text{Ar}$ complex was optimized using the same source configuration but with the use of pure Ar in the primary expansion rather than the H_2/Ar mixture. The cluster ion likely forms by charge-transfer collisions with larger Ar_n^+ clusters.

Size-selected clusters were then excited with a tunable IR OPO/OPA laser (*Laser Vision*) that generates light in the 800 – 3800 cm^{-1} range [11]. The change in mass associated with photoinduced Ar loss was recorded as a function of laser energy to generate action spectra:



The reported spectra typically result from addition of five individual scans, and are normalized to the laser output energy at each wavelength.

As mentioned above, the structures and harmonic spectra of the Im_nH^+ complexes have been reported earlier [13–16], and we have carried out a series of calculations in this work to access features of the potential surfaces not explicitly available from the previous papers. The results of our calculations are quantitatively consistent

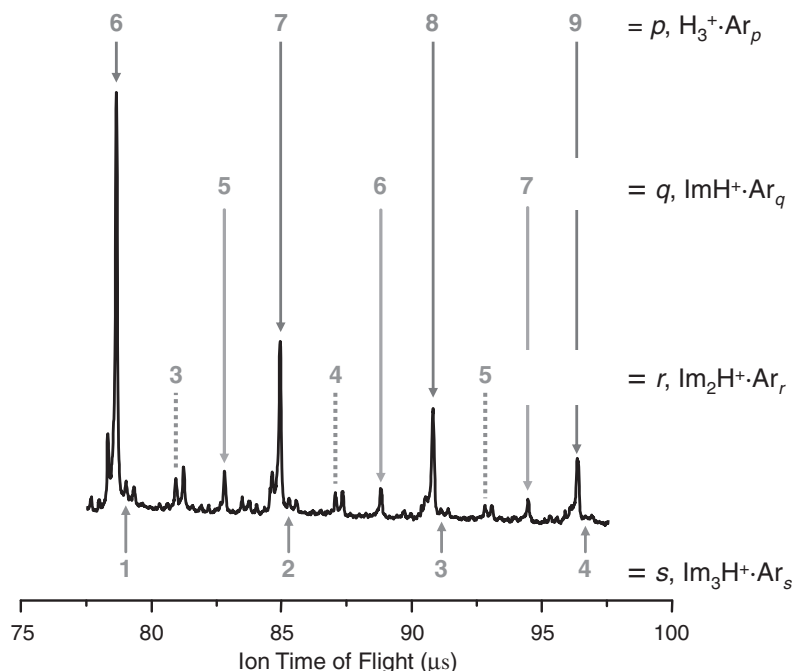


Figure 3. Mass spectrum illustrating the synthesis of Ar-tagged, protonated imidazole clusters by entrainment of imidazole into a beam of $\text{H}_3^+ \cdot \text{Ar}_s$ (top labels).

with the structural parameters and frequencies obtained previously. Our calculations were carried out using the GAUSSIAN03 package [20], where the minimum-energy structures for Im^+ and ImH^+ were generated at the MP2 level with aug-cc-pVTZ basis set and are shown in Figure 1. Harmonic vibrational spectra were calculated at the B3LYP level for all species with basis sets chosen according to those used in previous theoretical explorations of these systems (see Tables 1 and 2 for details). The C–H and the N–H stretching fundamentals were scaled by the anharmonicity factor appropriate to the level of theory (0.9682 for B3LYP 6-311G(d,p)) in accordance with the recommendation of Radom and co-workers [21]. The Ar-binding motifs in imidazolium were calculated at the MP2 level with basis set 6-311G(3df, 3pd) which recovered two local minima: one with the Ar bound to the ring and the other bound to the N–H group, with binding energies 0.9 and 5.3 kJ/mol respectively. However, upon correction for the basis set superposition error (BSSE), only the H-bonded form was found to be stable, with an Ar binding energy of 1.4 kJ/mol.

3. Results and discussion

3.1. Comparison of $\text{Im}^+ \cdot \text{Ar}$ and $\text{ImH}^+ \cdot \text{Ar}$

3.1.1. $\text{Im}^+ \cdot \text{Ar}$

Figure 4 presents a comparison of the Ar-tagged spectra of the Im^+ and ImH^+ ions. Two groups of bands appear, one near 3100 cm^{-1} arising from the C–H stretching fundamentals, and another near 3400 cm^{-1} associated with the N–H stretches. We note that the N–H stretching spectrum of Ar-tagged Im^+ has been previously reported by Dopfer and co-workers (along with that of the N_2 -tagged complex) using infrared photodissociation (IRPD) [13]. While their study recovered rather diffuse bands over the 3350 to 3450 cm^{-1} range, the spectrum acquired here is dominated by a narrow N–H feature at 3361 cm^{-1} . Another difference in the two spectra involves the C–H stretching region. Whereas the previous study did not recover any C–H activity for the $\text{Im}^+ \cdot \text{Ar}$ complex, our spectrum displays a clear feature in the C–H stretching region, with the strongest band appearing at 3130 cm^{-1} (Table 1). The

latter band is, however, quite close to the C–H fundamental identified in the $\text{Im}^+ \cdot \text{N}_2$ spectrum (3128 cm^{-1}), which was also reported in the earlier work [13].

The diffuse bands observed earlier for $\text{Im}^+ \cdot \text{Ar}$ [13] were discussed in the context of two stable isomers recovered in their *ab initio* calculations at the MP2 level (6-311G(2df,2pd)), where the Ar bound to the N–H group was found to be more stable than the ring- (or π -) bound form by 2.0 kJ/mol (167 cm^{-1}). Figure 4a presents the calculated harmonic spectrum for the structure displayed in the inset in Figure 4a, which is consistent with literature values [13,14] as reported in Table 1. The broad N–H structure observed earlier was attributed to both H- and π -bound isomeric forms that were present in comparable abundance. The sharp band in the present spectrum (Figure 4b) therefore indicates preferential formation of the H-bonded isomer, consistent with behavior expected for colder conditions in the ion source.

While the N–H stretching fundamental in $\text{Im}^+ \cdot \text{Ar}$ occurs significantly below the transition in isolated, neutral Im (3518 cm^{-1} , dashed gray line in Figure 4a) [22], the C–H stretches are only slightly red-shifted from those in neutral Im (3135 and 3160 cm^{-1}) [23]. The origin of these shifts is consistent with bond weakening upon electron removal and the red shift arising from Ar-attachment onto the most acidic N–H group as discussed previously [13].

3.1.2. $\text{ImH}^+ \cdot \text{Ar}$

Imidazolium is calculated to adopt the C_{2v} structure shown on the right in Figure 1, which is a symmetrical system featuring equivalent N–H bonds. Addition of an argon atom to one of these bonds should yield a widely split pair of N–H fundamentals in the predissociation spectrum (see harmonic spectrum in Figure 4d), and we indeed observe a strong doublet near 3450 cm^{-1} in the action spectrum (Figure 4c). The lower-energy transition at 3424 cm^{-1} corresponds to the Ar-bound N–H stretch, while the higher-energy peak (at 3469 cm^{-1}), which lies closer to the N–H stretching transition in neutral imidazole, is associated with the free (non-Ar-tagged) N–H stretch. The magnitude of this splitting (45 cm^{-1}) is on the same order as that recovered in a study of the $\text{ImH}^+ \cdot \text{N}_2$ complex by Adesokan et al. [24] where they report a

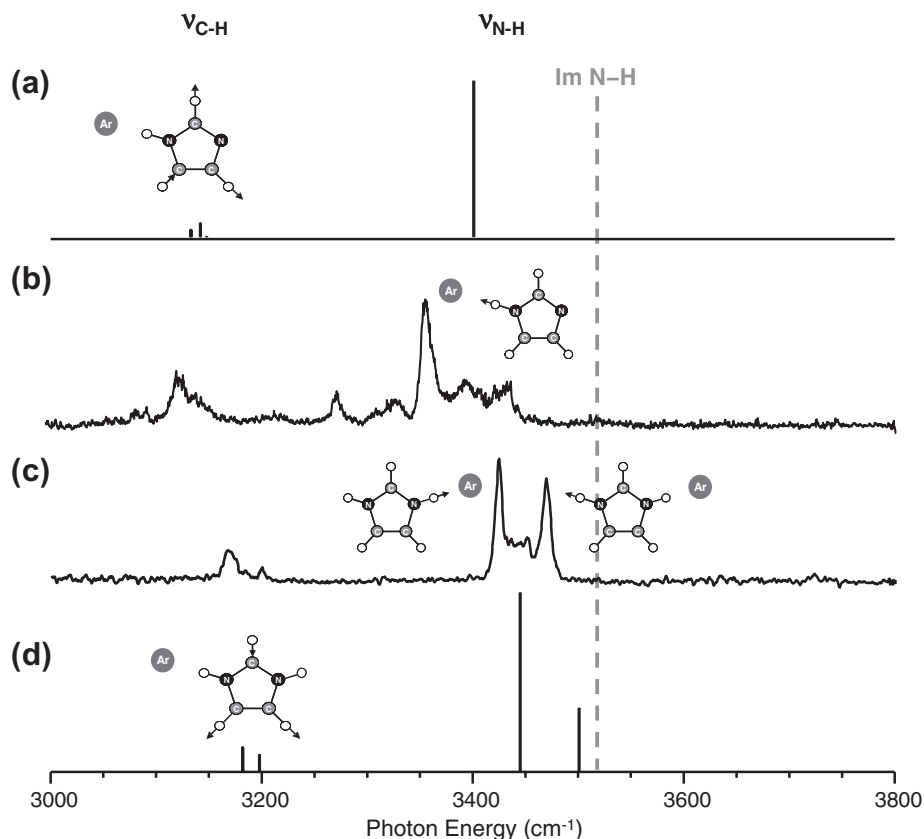


Figure 4. Comparison of vibrational spectra of $\text{Im}^+\cdot\text{Ar}$ and $\text{ImH}^+\cdot\text{Ar}$: (a) calculated harmonic spectrum of $\text{Im}^+\cdot\text{Ar}$ (H-bound) from literature [13], (b) experimental spectrum of $\text{Im}^+\cdot\text{Ar}$ with inset (*) showing comparison of our spectrum (bottom) with Ref. [13] IRPD spectrum (top) (c) experimental spectrum of $\text{ImH}^+\cdot\text{Ar}$, and (d) calculated harmonic spectrum of $\text{ImH}^+\cdot\text{Ar}$ (H-bound) recovered in this work at the B3LYP level with the 6-311G(2df,2pd) basis set and scaled by a factor of 0.9682(21). Representative motions responsible for the features are indicated by displacement vectors in the minimum-energy structures. The N–H stretching frequency of neutral Im is marked by a dashed gray line.

Table 1

Vibrational bands obtained by infrared photodissociation (IRPD) ($\pm 5 \text{ cm}^{-1}$) for $\text{Im}^+\cdot\text{Ar}$ and $\text{ImH}^+\cdot\text{Ar}$ with comparison of theoretical values of Im^+ and ImH^+ fundamentals.

Species	Method	Transition energies (cm^{-1})		
		C–H Stretches	N–H·Ar Stretch	Free N–H Stretch
$\text{Im}^+\cdot\text{Ar}(\text{H})$	IRPD (this work)	3088, 3130	3361	
	IRPD (13)		3361	
	B3LYP/6-311G(2df,2pd) (13)	3110, 3118 , 3124	3362	
$\text{Im}^+\cdot\text{Ar}(\pi)$	IRPD (13)			3433
	B3LYP/6-311G(2df,2pd) (13)	3111, 3118 , 3127		3432
Im^+	B3LYP/6-311G(2df,2pd) (13)	3109, 3116 , 3122		3430
	$\text{ImH}^+\cdot\text{Ar}$	IRPD (this work)	3168	3469
ImH^+	IRPD (14)			~ 3470
	B3LYP/6-311G(2df,2pd) ^a	3182 ^b , 3198	3445	3501
	B3LYP/6-311G(2df, 2pd) ^a	3182 ^b , 3197		3495 ^{as} , 3503 ^s
	MP2/6-311G(2df,2pd) (14)			3467 ^{as} , 3474 ^s

^a Transition energies are scaled by the factor 0.9682 as tabulated in Ref. [21].

^b Transition energy referring to two nearly degenerate ($<1 \text{ cm}^{-1}$) vibrational modes. Numbers in bold face indicate the most intense C–H stretch for the system. Superscripts 's' and 'as' refer to symmetric and asymmetric N–H stretches, respectively.

free N–H stretching frequency 66 cm^{-1} higher in energy than that complexed to the N_2 ligand. In the lower-energy regions of the spectra in Figure 4, we also notice a trend in the C–H stretching features in that they are significantly blue-shifted from Im^+ to ImH^+ (by $\sim 40 \text{ cm}^{-1}$). This blue shift can be rationalized as before [13] by the redistribution of excess positive charge away from the ring, strengthening the C–H and N–C bonds as the charge density becomes more similar to that in neutral Im.

3.1.3. $\text{Im}_2\text{H}^+\cdot\text{Ar}$

The nature of the intermolecular proton bond formed between Im and ImH^+ was considered in a 2003 computational study by Tatara et al. [15] in which they performed a relaxed potential energy surface scan along the proton-transfer coordinate. This procedure recovered two shallow isoenergetic minima separated by an energy barrier of 200 cm^{-1} . They noted, however, that the vibrational zero-point energy of the complex was larger than the barrier

height, leading them to suggest that ‘classical motion of the proton between the two molecules is allowed’.

Figure 5c presents the experimental spectrum of $\text{Im}_2\text{H}^+\cdot\text{Ar}$ in the high frequency region of the N–H and C–H stretches. While the C–H stretching features in $\text{ImH}^+\cdot\text{Ar}$ are essentially unaffected by addition of Im, its open N–H stretching doublet evolves into a single dominant band in $\text{Im}_2\text{H}^+\cdot\text{Ar}$ at 3492 cm^{-1} . This is consistent with formation of a symmetrical structure as suggested by Tataru et al. [15], which is calculated to yield very little splitting ($<1\text{ cm}^{-1}$) between the dangling N–H groups. The sharp band occurs with a substantial blue shift (23 cm^{-1}) of this single dominant N–H feature compared with the free N–H stretching frequency in the $\text{ImH}^+\cdot\text{Ar}$ complex. The shift to higher energy leads us to conclude that the excess charge becomes more localized along the bridging proton, allowing the uncomplexed N–H groups to adopt structures closer to that in neutral Im.

Im_2H^+ appears to present a similar case to that found in the N_2H_7^+ [25] complex (another double-minimum situation), where the appearance of equivalent NH_3 groups was explained by effective averaging over large amplitude zero-point motion of the bridging proton. In that case, the ZPE of the one-dimensional H-atom motion was found to lie above the barrier. We note that there is a weak shoulder on the low energy side of the sharp band in the Im_2H^+ spectrum (Figure 5c) which could in principle arise from possible asymmetric binding of the Ar. Because it is likely that this system involves a delocalized, large amplitude intermolecular proton bond, however, we did not carry out an extensive survey to identify the preferred binding site of the Ar atom, as this would require inclusion of nuclear quantum effects along with high-level electronic structure theory [26]. Moreover, since we are primarily interested in characterizing the intermolecular proton bond, we turned to experiment in order to identify the transitions directly arising from the motion of the bridging proton.

To estimate the location of the bridging proton transitions in Im_2H^+ , we invoked a one-dimensional sinc-DVR approach [27]. This method recovered the levels arising from H atom motion (unit mass) confined to the double-minimum potential surface along the N–H–N coordinate. The surface was sampled in increments of 0.1 \AA and calculated at the B3LYP 6-311G(d,p) level, yielding a similar barrier (192 cm^{-1}) and equilibrium N–N bond length (2.66 \AA) as those reported previously [15]. This procedure predicts the fundamental for the asymmetric N–H–N stretch to occur at 822 cm^{-1} , so that the one-dimensional zero-point level (401 cm^{-1}) determined in our calculation indeed lies above the barrier. The zero-point level, wavefunction, and shape of the surface are included as in inset in Figure 6.

The experimental vibrational predissociation spectrum of the $\text{Im}_2\text{H}^+\cdot\text{Ar}$ complex in the low frequency region anticipated for the bridging proton is presented in Figure 6. Most importantly, this spectrum is dominated by a very strong, nearly symmetrical doublet with peaks at 1014 and 1061 cm^{-1} . This behavior is quite reminiscent of that found in a large number of binary proton bound complexes [11,25] in which the parallel stretch of the bridging proton frequently occurs as a doublet that dominates this spectral region (again near 1000 cm^{-1}) with similar splittings to that observed here. We therefore associate the strong doublet found in the Im_2H^+ complex to shared proton activity, which falls about 200 cm^{-1} higher in frequency than the simple 1-D anharmonic prediction (822 cm^{-1}). Note that the observed location lies far below the harmonic value (2049 cm^{-1} , Table 2) [15], which corresponds to the curvature of the surface at the global-minimum structure (Figure 2a). In the case of the O–H⁺–O linkages discussed earlier [11], the doublet structure was rationalized in the context of mixing with the nearby C–O stretching modes, which has the effect of diluting the large intrinsic intensity associated with parallel stretch of the bridging proton. In the present case, we note

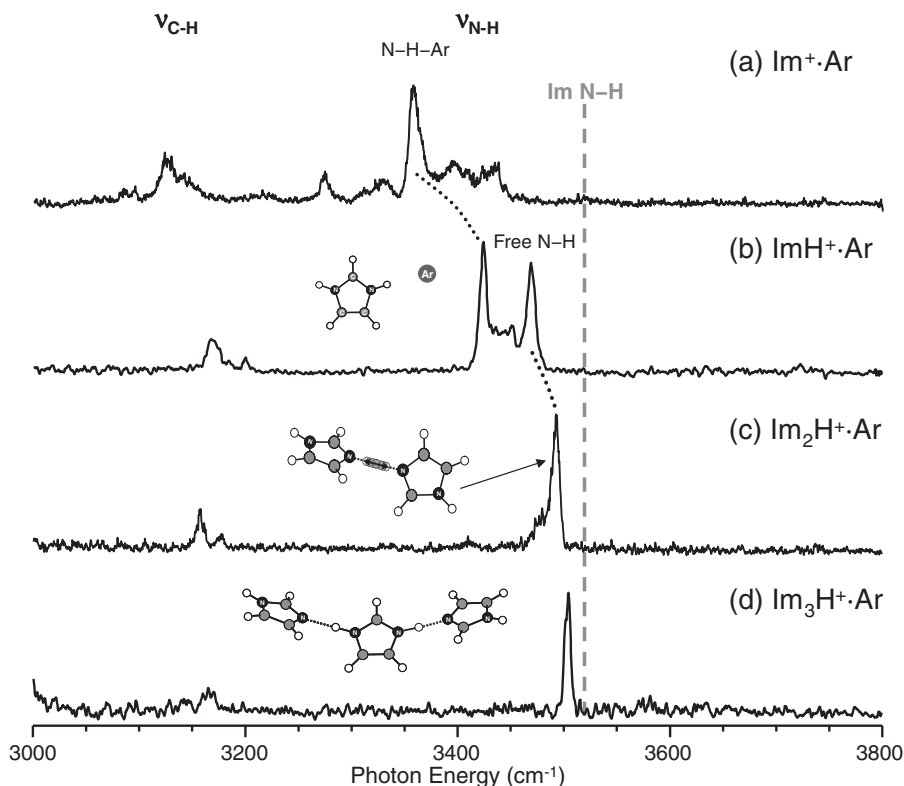


Figure 5. Vibrational predissociation spectra of (a) $\text{Im}^+\cdot\text{Ar}$, (b) $\text{ImH}^+\cdot\text{Ar}$, (c) $\text{Im}_2\text{H}^+\cdot\text{Ar}$, and (d) $\text{Im}_3\text{H}^+\cdot\text{Ar}$, which outline the systematic blue shift of the terminal N–H stretching frequencies toward that of neutral imidazole (dashed gray line) as the chain length increases.

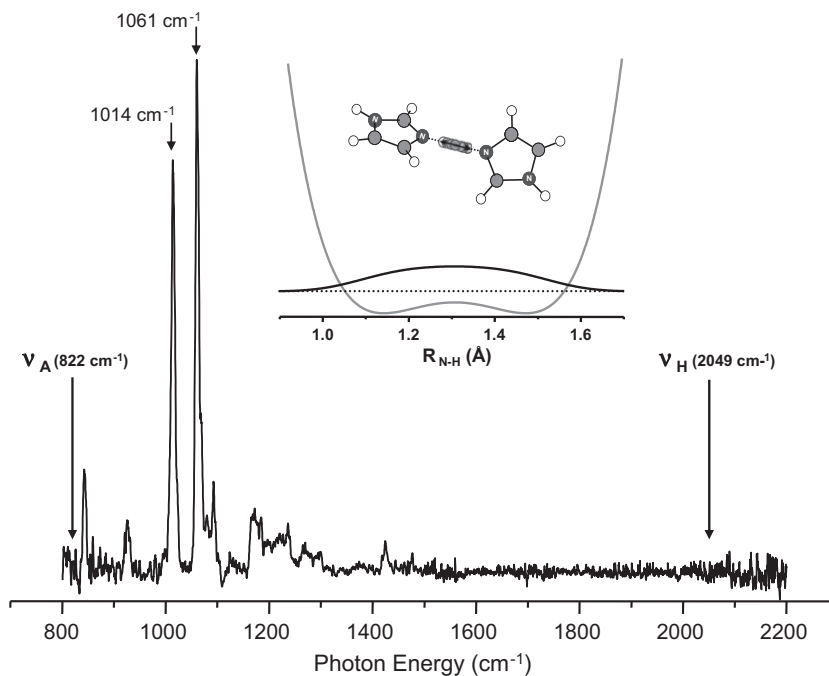


Figure 6. Vibrational predissociation spectrum of $\text{Im}_2\text{H}^+\cdot\text{Ar}$ in the lower frequency region ($800\text{--}2200\text{ cm}^{-1}$) where transitions are expected for the parallel stretch associated with the bridging proton. The inset shows the calculated potential energy surface along the proton-transfer coordinate. Arrows indicate the positions of the calculated anharmonic (ν_A , see text for details) and harmonic (ν_H) stretching frequencies reported in Table 2.

Table 2

Vibrational bands obtained by infrared photodissociation (IRPD) ($\pm 5\text{ cm}^{-1}$) for $\text{Im}_n\text{H}^+\cdot\text{Ar}$, $n = 2\text{--}3$, with comparison of theoretical values of Im_nH^+ , $n = 2\text{--}3$ fundamentals.

Species	Method	Transition energies (cm^{-1})			
		C–H Stretches	N–H–N Stretch	N–H–Ar Stretch	Free N–H Stretch
$\text{Im}_2\text{H}^+\cdot\text{Ar}$	IRPD (this work)	3154, 3177	1014, 1061		3492
$\text{Im}_2\text{H}^+\cdot\text{Ar}$ (min. energy struct.)	B3LYP/6-311G(d,p) ^a	3156, 3159, 3175, 3178, 3182, 3193		3488	3524
Im_2H^+ (min. energy struct.)	B3LYP/6-311G(d,p) ^a	3156, 3160, 3175, 3178, 3183, 3192	1934		3512, 3524
	B3LYP/6-311++G** (15)	3259, 3263, 3278, 3282, 3287, 3296	2049		3626, 3638
Im_2H^+ (relaxed PES scan)	Sinc-DVR		822		
Im_2H^+ (transition state)	B3LYP/6-311G(d,p) ^a	3166, 3169, 3187	i766		3518
	B3LYP/6-311++G** [15]	3269, 3272, 3290	i796		3632
$\text{Im}_3\text{H}^+\cdot\text{Ar}$	IRPD (this work)	3143, 3168			3503
Im_3H^+ (relaxed PES scan)	sinc-DVR		1969		
Im_3H^+ (min. energy struct.)	B3LYP/6-311G(d,p) ^a	3152, 3156, 3173, 3178, 3180, 3191	2430 ^{as} , 2526 ^s		3529
	B3LYP/6-311+G* [16]		2673 ^{as} , 2752 ^s		3648

^a Transition energies recovered in this work are scaled by the anharmonicity factor 0.9682 as tabulated in Ref. [21] while literature values are not scaled. Superscripts “s” and “as” refer to symmetric and asymmetric N–H stretches, respectively.

that there are two C–N stretching bands calculated to occur near the observed doublet ($1140\text{--}1182\text{ cm}^{-1}$) [15] which could play a similar role. This tentative assignment scheme can be critically evaluated by exploring the H/D isotope dependence of the band, and these experiments are an obvious next step in the characterization of these important species.

3.1.4. $\text{Im}_3\text{H}^+\cdot\text{Ar}$

The predissociation spectrum of the Ar-tagged Im_3H^+ cluster is displayed in Figure 5d. The weak C–H transitions occur at essentially the same positions throughout the series. Therefore, we focus our attention on the single sharp peak in the vicinity of the N–H stretch at 3503 cm^{-1} , lying just 15 cm^{-1} below the N–H stretch in neutral Im (3518 cm^{-1}). This experimental result agrees with the theoretical prediction [16] that the trimer adopts the symmetrical structure indicated in the inset, where the observed band arises from the nearly degenerate symmetric and asymmetric stretching bands on the free N–H groups. Note that the theoretical (harmonic) splitting for these modes is less than 1 cm^{-1} in the isolated Im_3H^+ cluster

and the dominant transition that derives from the equivalent N–H groups corresponds to the asymmetric stretch. The fact that only a single peak is observed indicates that the Ar atom does not substantially perturb the core ion.

The symmetrical structure predicted for the trimer is interesting in that it corresponds to a ‘double bridge’ involving two nominal intermolecular proton bonds. As such, each bridging bond has a smaller excess charge density than in the case of the binary intermolecular proton bond, and one suspects that this should act to blue-shift the stretches associated with the collective motions of both bridging protons. Experimental observation of these lower energy bands in the trimer and larger clusters is a clear target for future studies of this system.

4. Summary

We report the spectral evolution of the C–H and N–H fundamentals in the proton bound complexes of imidazole Im_nH^+ , obtained using mass-selective Ar-tagging predissociation spectroscopy. The

exterior N–H stretching transitions display incremental blue shifts toward the N–H stretch in neutral imidazole, with the value in the $n = 3$ case falling only 15 cm^{-1} below the neutral transition. The spectral signature of the bridging proton is identified in the $n = 2$ complex as a very intense doublet near 1000 cm^{-1} , split by about 50 cm^{-1} . This observation, in conjunction with 1-D anharmonic calculations, indicates that the zero-point motion of the bridging proton lies above the calculated barrier for intra-cluster proton transfer.

Acknowledgments

We thank the Division of Chemistry of the National Science Foundation, CHE-091199, as well as the NSF 'Fueling the Future' Center for Chemical Innovation (CHE-0739227), for support of this work. We thank Christopher M. Leavitt for valuable theoretical assistance in numerous aspects of this work.

References

- [1] J. Sasaki, J.L. Spudich, *Biophys. J.* 77 (1999) 2145.
- [2] X. Chen, J.L. Spudich, *J. Biol. Chem.* 279 (2004) 42964.
- [3] K.D. Kreuer, *J. Membrane. Sci.* 185 (2001) 29.
- [4] J. Thomas et al., *J. Electrochem. Soc.* 140 (1993) 1041.
- [5] T.E. Springer, T.A. Zawodzinski, S. Gottesfeld, *J. Electrochem. Soc.* 138 (1991) 2334.
- [6] M. Rikukawa, K. Sanui, *Prog. Polym. Sci.* 25 (2000) 1463.
- [7] N. Solca, O. Dopfer, *J. Am. Chem. Soc.* 126 (2004) 9520.
- [8] S. Bureekaew et al., *Nat. Mater.* 8 (2009) 831.
- [9] H. Chen, T. Yan, G.A. Voth, *J. Phys. Chem. A* 113 (2009) 4507.
- [10] E.S. Stoyanov, C.A. Reed, *J. Phys. Chem. A* 110 (2006) 12992.
- [11] J.R. Roscioli, L.R. McCunn, M.A. Johnson, *Science* 316 (2007) 249.
- [12] W.H. Robertson, M.A. Johnson, *Rev. Sci. Instrum.* 71 (2000) 4431.
- [13] H.-S. Andrei, N. Solca, O. Dopfer, *J. Phys. Chem. A* 109 (2005) 3598.
- [14] H.-S. Andrei, N. Solca, O. Dopfer, *ChemPhysChem* 7 (2006) 107.
- [15] W. Tataru, M.J. Wojcik, J. Lindgren, M. Probst, *J. Phys. Chem. A* 107 (2003) 7827.
- [16] S. Yan, Y. Bu, P. Li, *J. Chem Phys.* 122 (2005) 054311.
- [17] E.J. Bieske, O. Dopfer, *Chem. Rev.* 100 (2000) 3963.
- [18] E.P.L. Hunter, S.G. Lias, *J. Phys. Chem. Ref. Data* 27 (1998) 413.
- [19] L.A. Posey, M.A. Johnson, *J. Chem. Phys.* 89 (1988) 4807.
- [20] M.J. Frisch et al., GAUSSIAN 03, Revision C.02, GAUSSIAN Inc., Wallingford, CT, 2004.
- [21] J.P. Merrick, D. Moran, *J. Phys. Chem. A* 111 (2007) 11683.
- [22] M.Y. Choi, *J. Phys. Chem. A* 110 (2006) 9344.
- [23] S.-T. King, *J. Phys. Chem* 74 (1970) 2133.
- [24] A. Adesokan, G. Chaban, O. Dopfer, R. Gerber, *J. Phys. Chem. A* 111 (2007) 7374.
- [25] K.R. Asmis et al., *Angew. Chem. Int. Ed.* 46 (2007) 8691.
- [26] S.P. Webb, T. Iordanov, S. Hammes-Schiffer, *J. Chem. Phys.* 117 (2002) 4106.
- [27] D.T. Colbert, W.H. Miller, *J. Chem. Phys.* 96 (1992) 1982.